Direct detection of pNG dark matter in the S2HDM

Pedro Gabriel (CFTC-UL/ITP-KIT)

In collaboration with: Thomas Biekötter, Maria Olalla Olea Romacho and Rui Santos

Workshop on Multi-Higgs Models

Lisbon, September 2024

Fundação para a Ciência e a Tecnologia

Funded by FCT in the framework of projects no. CFTC: UIDB/00618/2020, UIDP/00618/2020 and grant no. 2022.11377.BD

Motivation

Dark matter (DM) remains one of the greatest enigmas in modern physics, despite nearly a century of indirect evidence and ongoing theoretical and experimental efforts.

Numerous experiments are actively searching for direct evidence of dark matter. Leading DM direct detection experiments like PandaX-4T, XENON1T, and LZ have set stringent limits on the properties of WIMPs, pushing the boundaries of our understanding and guiding new theoretical models.

Pseudo-Nambu-Goldstone (pNG) DM models introduce a complex singlet field under a softly broken global U(1) symmetry. These models have been shown to produce vanishing tree-level direct detection cross-sections and rely on one-loop electroweak corrections for detectable signals, which can align with current and future experimental sensitivities

[Gross, Lebedev, Toma, 2017] [Ishiwata, Toma, 2018] [Azevedo, Duch, Grzadkowski, Huang, Iglicki, Santos, 2019] [Glaus, Mühlleitner, Müller, Patel, Römer, Santos, 2020]

Goal: Calculate the radiative corrections to the DM direct detection cross-section in the S2HDM with pNG DM and check if it would be possible to probe the parameter space in current or future experiments.

[T. Biekötter, P. Gabriel, M. O. Olea-Romacho, R. Santos, "Direct detection of pseudo-Nambu-Goldstone dark matter in a two Higgs doublet plus singlet extension of the SM", JHEP 10(2022), 126. [arXiv:2207.04973]]

S2HDM with pNG DM

Scalar potential

$$V = \mu_{11}^2|\phi_1|^2 + \mu_{22}^2|\phi_2|^2 - \mu_{12}^2\left(\phi_1^\dagger\phi_2 + \phi_2^\dagger\phi_1\right) + \frac{\lambda_1}{2}|\phi_1|^4 + \frac{\lambda_2}{2}|\phi_2|^4 + \lambda_3|\phi_1|^2|\phi_2|^2 + \lambda_4\left(\phi_1^\dagger\phi_2\right)\left(\phi_2^\dagger\phi_1\right)$$
$$+\frac{\lambda_5}{2}\left(\left(\phi_1^\dagger\phi_2\right)^2 + \left(\phi_2^\dagger\phi_1\right)^2\right) + \frac{\mu_S^2}{2}|\phi_S|^2 + \frac{\lambda_6}{2}|\phi_S|^4 + \lambda_7|\phi_1|^2|\phi_S|^2 + \lambda_8|\phi_2|^2|\phi_S|^2 \boxed{-\frac{\mu_\chi^2}{4}\left(\phi_S^2 + (\phi_S^*)^2\right)}$$

soft-breaking term

Fields

$$\phi_1 = \begin{pmatrix} \phi_1^+ \\ \frac{v_1 + \rho_1 + i\sigma_1}{\sqrt{2}} \end{pmatrix}$$

$$\phi_2 = \begin{pmatrix} \phi_2^+ \\ \frac{v_2 + \rho_2 + i\sigma_2}{\sqrt{2}} \end{pmatrix}$$

$$\phi_S = \frac{v_S + \rho_2 + i\chi}{\sqrt{2}}$$

DM candidate

Rotation to the mass basis

$$\begin{pmatrix} h_a \\ h_b \\ h_c \end{pmatrix} = \boxed{\begin{pmatrix} c_{\alpha_1}c_{\alpha_2} & s_{\alpha_1}c_{\alpha_2} & s_{\alpha_2} \\ -(s_{\alpha_1}c_{\alpha_3} + c_{\alpha_1}s_{\alpha_2}s_{\alpha_3}) & c_{\alpha_1}c_{\alpha_3} - s_{\alpha_1}s_{\alpha_2}s_{\alpha_3} & c_{\alpha_2}s_{\alpha_3} \\ s_{\alpha_1}s_{\alpha_3} - c_{\alpha_1}s_{\alpha_2}c_{\alpha_3} & -(c_{\alpha_1}s_{\alpha_3} + s_{\alpha_1}s_{\alpha_2}c_{\alpha_3}) & c_{\alpha_2}c_{\alpha_3} \end{pmatrix}} \begin{pmatrix} \rho_1 \\ \rho_2 \\ \rho_S \end{pmatrix}$$

R

$$\begin{pmatrix} G^+ \\ H^+ \end{pmatrix} = U\begin{pmatrix} \phi_1^+ \\ \phi_2^+ \end{pmatrix} \qquad \begin{pmatrix} G^0 \\ A \end{pmatrix} = U\begin{pmatrix} \sigma_1 \\ \sigma_2 \end{pmatrix} \qquad U = \begin{pmatrix} c_\beta & -s_\beta \\ s_\beta & c_\beta \end{pmatrix}$$

$$\{m_{h_a}^2, m_{h_b}^2, m_{h_c}^2, m_{h_\pm}^2, m_A^2, m_\chi^2, v, v_S, \alpha_1, \alpha_2, \alpha_3, \tan(\beta), \mu_{12}^2\}$$

[Jiang, Cai, Yu, Zeng, Zhang, 2019]

1-loop corrected DM-nucleon cross-section

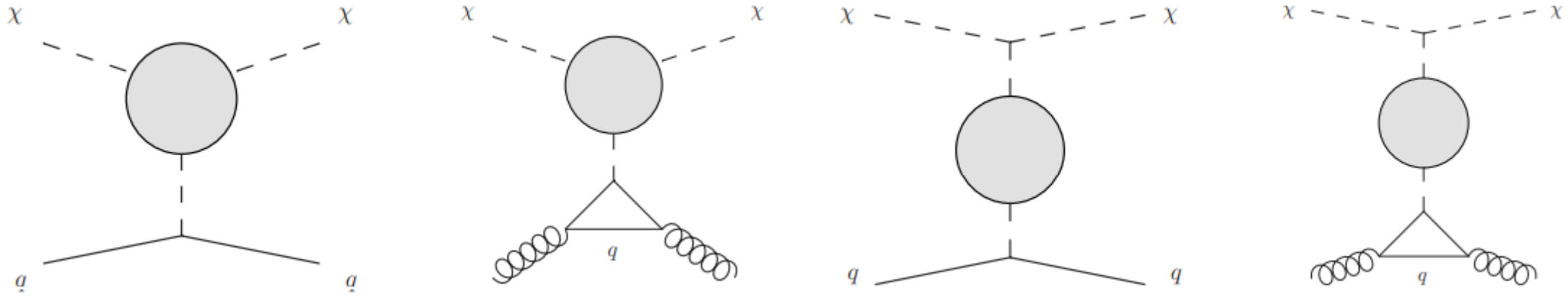

$$\mathcal{L}_{\text{eff}} = m_q C_q^S \chi\chi\bar{q}q \qquad m_Q \bar{Q}Q \to -\frac{\alpha_s}{12\pi} G_{\mu\nu}G^{\mu\nu}$$

$$\sigma_{\chi N} = \frac{m_N^4}{\pi\left(m_N + m_\chi\right)^2}\left|\sum_{q=u,d,s} C_q^S f_{T_q}^N + \frac{2}{27} f_{T_g}^N \sum_{q=b,c,t} C_q^S\right|^2$$

Type I/LS: $C_q^{I,LS} = C_{u,d,c,s,b,t}^S$

Type II/F: $C_u^{II,F} = C_{u,c,t}^S$

$C_d^{II,F} = C_{d,s,b}^S$

$$f_{Tu}^p = 0.029\ ,\ f_{Td}^p = 0.027\ ,\ f_{Ts}^p = 0.009$$
$$f_{Tu}^n = 0.013\ ,\ f_{Td}^n = 0.040\ ,\ f_{Ts}^n = 0.009$$

$$f_{T_g}^N = 1 - \sum_{q=u,d,s} f_{T_q}^N$$

Results

Order of magnitude of the radiative corrections

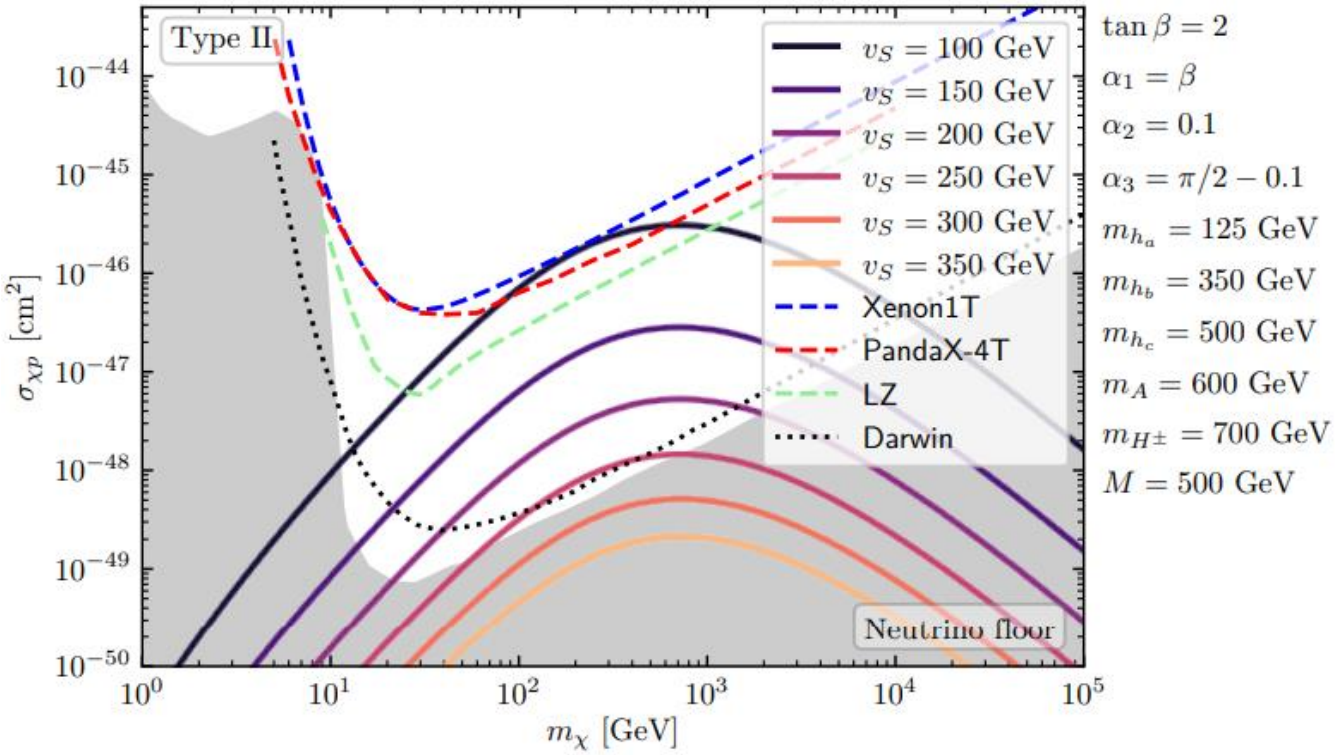

The loop corrected cross-section is within range of direct detection experiments.

In the limit when $m_\chi \to 0$, the direct detection cross-section goes to zero. This is due to the U(1) symmetry being restored, making the cross-section, in the limit $t \to 0$, vanish at all orders.

In the limit when $m_\chi \gg m_{h_i}$, the cross-section also decreases because it is proportional to $1/m_\chi$.

The maximum values for the cross-section are obtain for $m_\chi \approx m_{h_i}$.

Lower values of v_S produce higher cross-sections due to the portal couplings $(\lambda_6, \lambda_7, \lambda_8)$ being inversely proportional to v_S.

Results

Validity of the cancellation mechanism

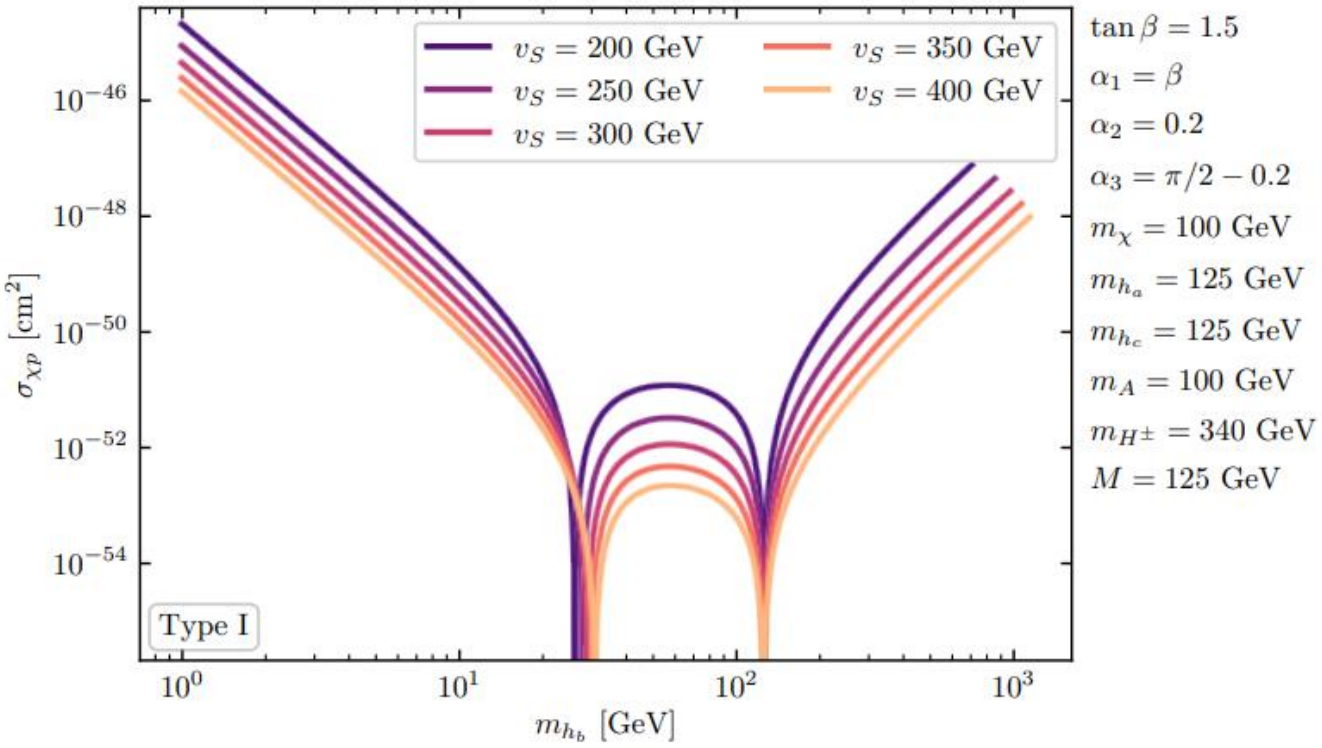

The cancellation mechanism when $t \to 0$ should only hold if all Higgs bosons have $m_h^2 \gg t$.

We observed that when $m_{h_b} \to 0$, the cross-section increases drastically as was expected.

When $m_{h_b} \gg m_\chi$, the cross-section also increases since the portal couplings $(\lambda_6, \lambda_7, \lambda_8)$ increase with the mass of the Higgs bosons.

"Blind-spots": regions where the cross-section drops to zero because of cancellations between loop diagrams.

Results

Cross-section suppression from Wilson coefficients

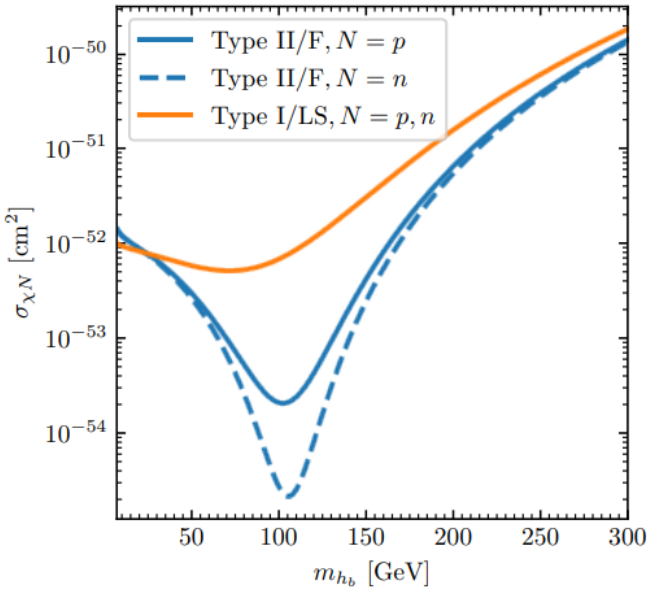

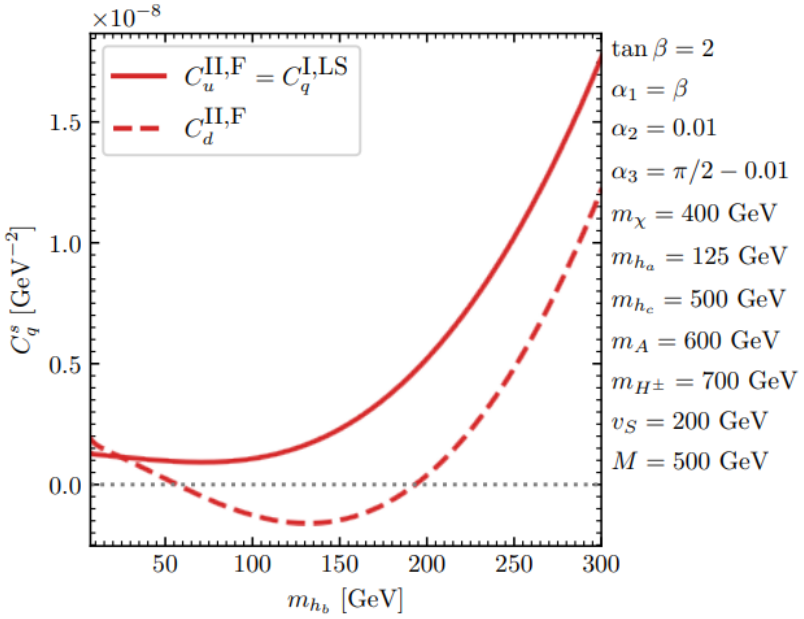

Depending on the 2HDM type, further cross-section suppression can occur due to cancellation in the sum over quark contributions.

Cross-section can drop by around 2 orders of magnitude between protons and neutrons in Type II/F.

This occurs because Type II/F has different Wilson coefficients for up and down-quarks.

When the coefficients have different signs, it leads to cross-section suppression.

Results

Parameter space scan

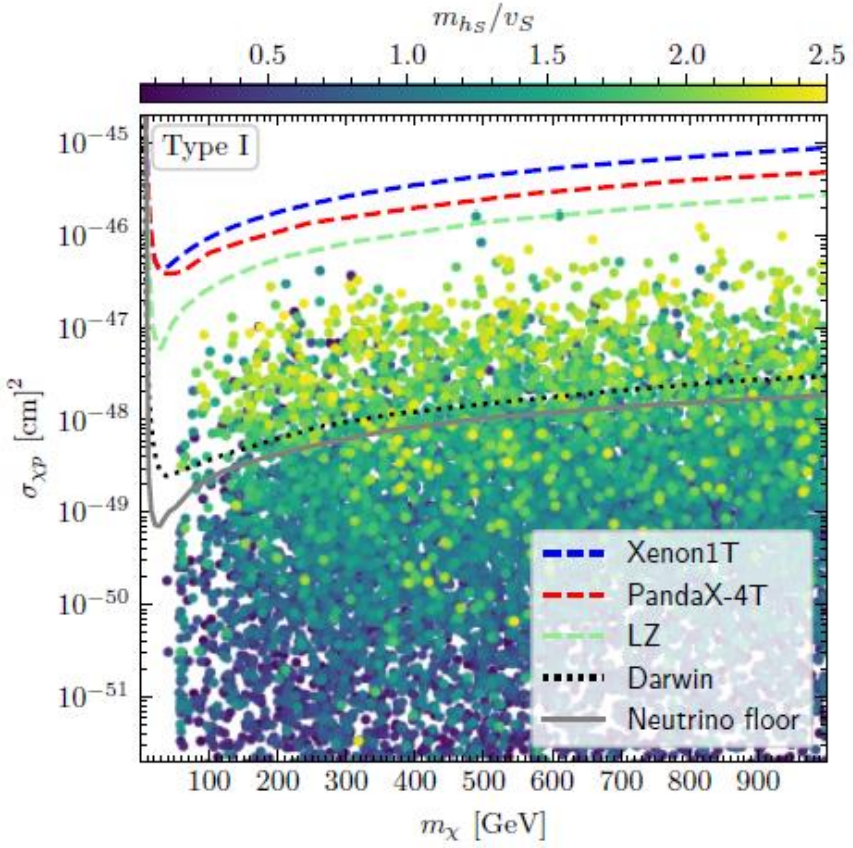

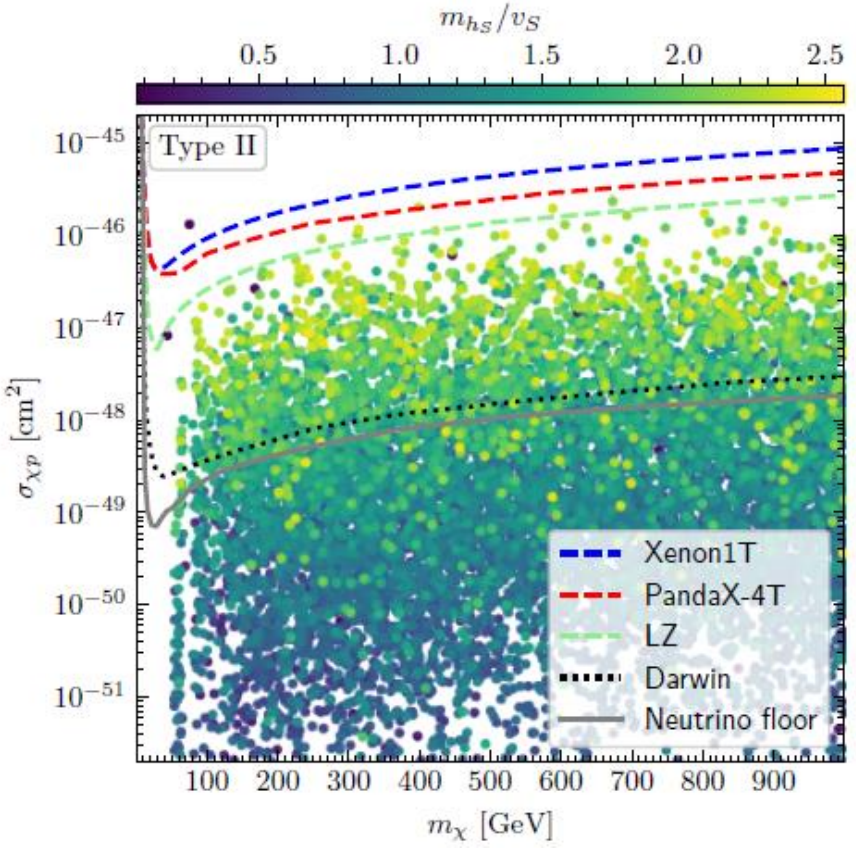

Results

Parameter space scan

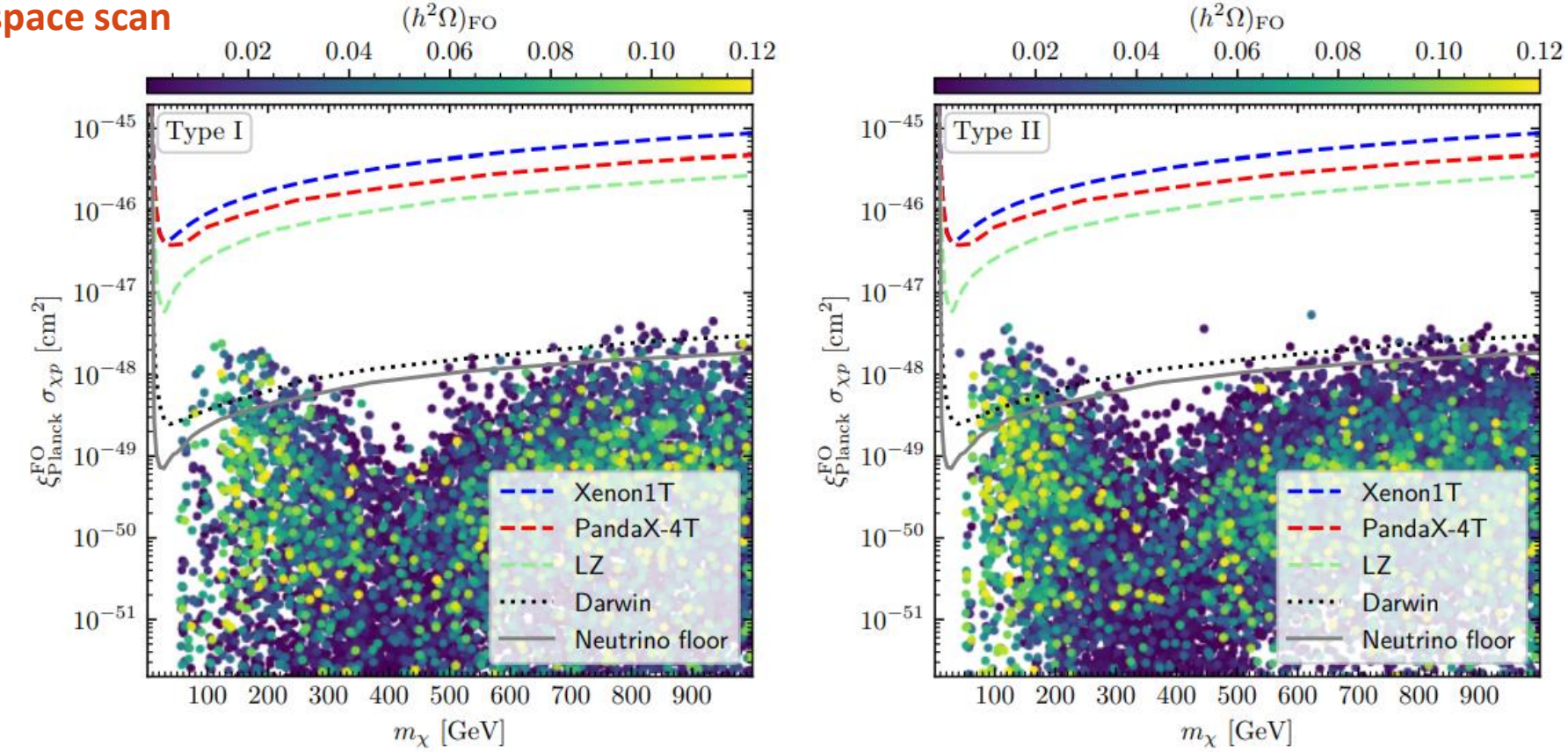

$$\xi^{FO}_{Planck} = \frac{(\Omega h^2)_{FO}}{(\Omega h^2)_{Planck}}$$

Conclusions

Calculated the radiative corrections for the DM-nucleon scattering in the S2HDM with a pNG DM candidate in the limit of vanishing momentum exchange.

Confirmed that the model respects the theoretical constraints in this limit and that the corrections at NLO have an order of magnitude within the range of current and future DM direct detection experiments.

Observed that some cross-section suppression may occur in Type II/F due to different Wilson coefficients for up and down-type quarks having different signs while this does not occur in Type I/LS. This could be a way for distinguish between the two types.

Performed a parameter space scan and observed that while current DM direct detection experiments can not probe the model's parameter space, some points for $60\ GeV \lesssim m_\chi \lesssim 300\ GeV$ are within the range of future experiments such as DARWIN.

Backup

Dark matter-nucleon scattering

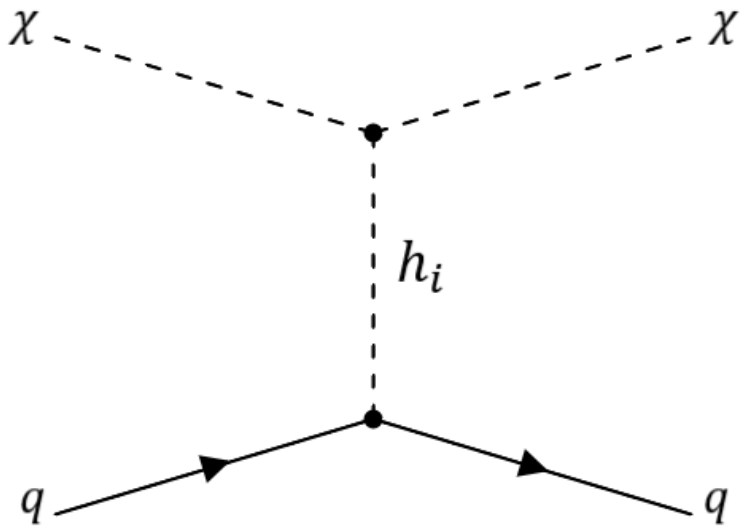

$$\Gamma_{h_i\chi\chi} = -(\lambda_7 v_1 R_{1i} + \lambda_8 v_2 R_{2i} + \lambda_6 v_S R_{3i})$$

$$i\mathcal{M}_{\chi q} = i\frac{Y_q}{\sqrt{2}}\bar{u}(k_2)u(k_1)\left(\frac{\Gamma_{h_1\chi\chi}}{t-m_{h_1}}R_{a1} + \frac{\Gamma_{h_2\chi\chi}}{t-m_{h_2}}R_{a2} + \frac{\Gamma_{h_3\chi\chi}}{t-m_{h_3}}R_{a3}\right)$$

$t \to 0$

$$-(\Gamma_{h_1\chi\chi} \quad \Gamma_{h_2\chi\chi} \quad \Gamma_{h_3\chi\chi})\left(M_h^2\right)^{-1}R^T(\delta_{a1} \quad \delta_{a2} \quad 0)^{\mathrm{T}}$$

$$(\lambda_7 v_1 \quad \lambda_8 v_2 \quad \lambda_6 v_S)\left(M_\rho^2\right)^{-1}(\delta_{a1} \quad \delta_{a2} \quad 0)^{\mathrm{T}} = 0$$

Type I/LS: $d, u \to a = 2$

Type II/F: $d \to a = 1$

$u \to a = 2$

$$\left(M_\rho^2\right)^{-1} = \mathrm{R}\left(\mathrm{M_h^2}\right)^{-1}\mathrm{R^T}$$

$$(\Gamma_{h_1\chi\chi} \quad \Gamma_{h_2\chi\chi} \quad \Gamma_{h_3\chi\chi}) = (\lambda_7 v_1 \quad \lambda_8 v_2 \quad \lambda_6 v_S)R$$

[Jiang, Cai, Yu, Zeng, Zhang, 2019]

Radiative corrections

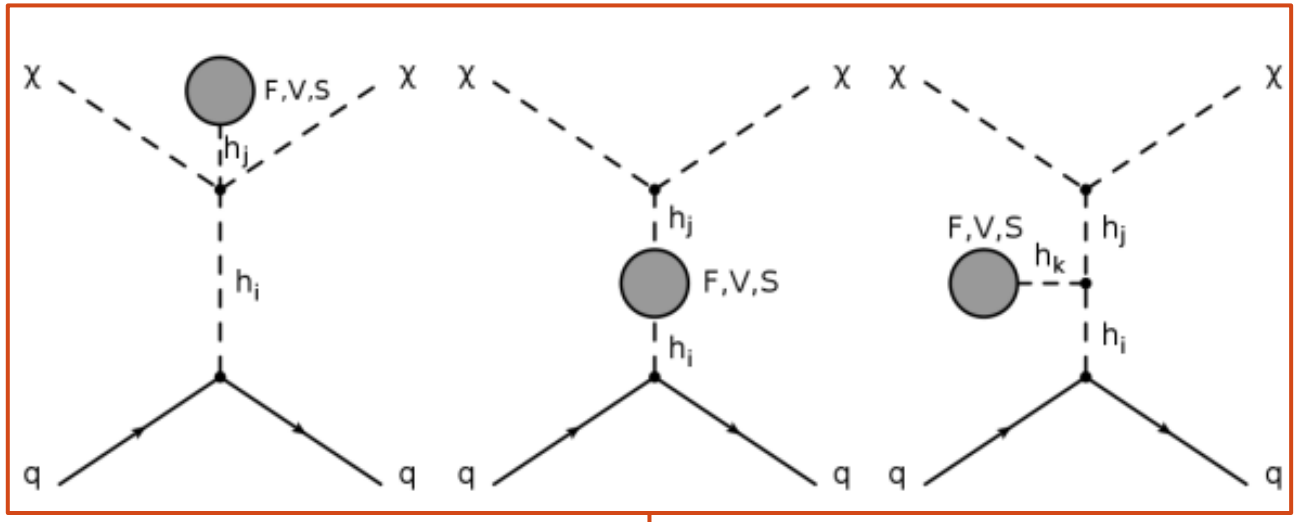

Contributions cancel between themselves

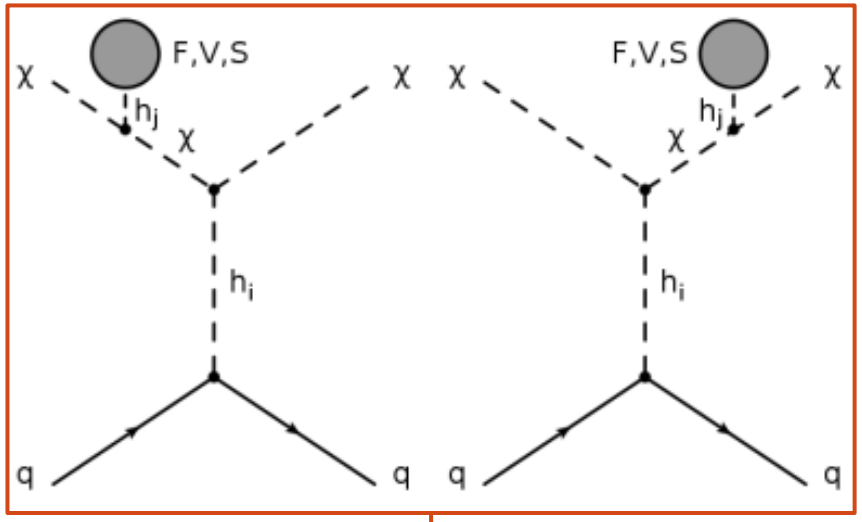

Proportional to tree-level amplitude

Radiative corrections

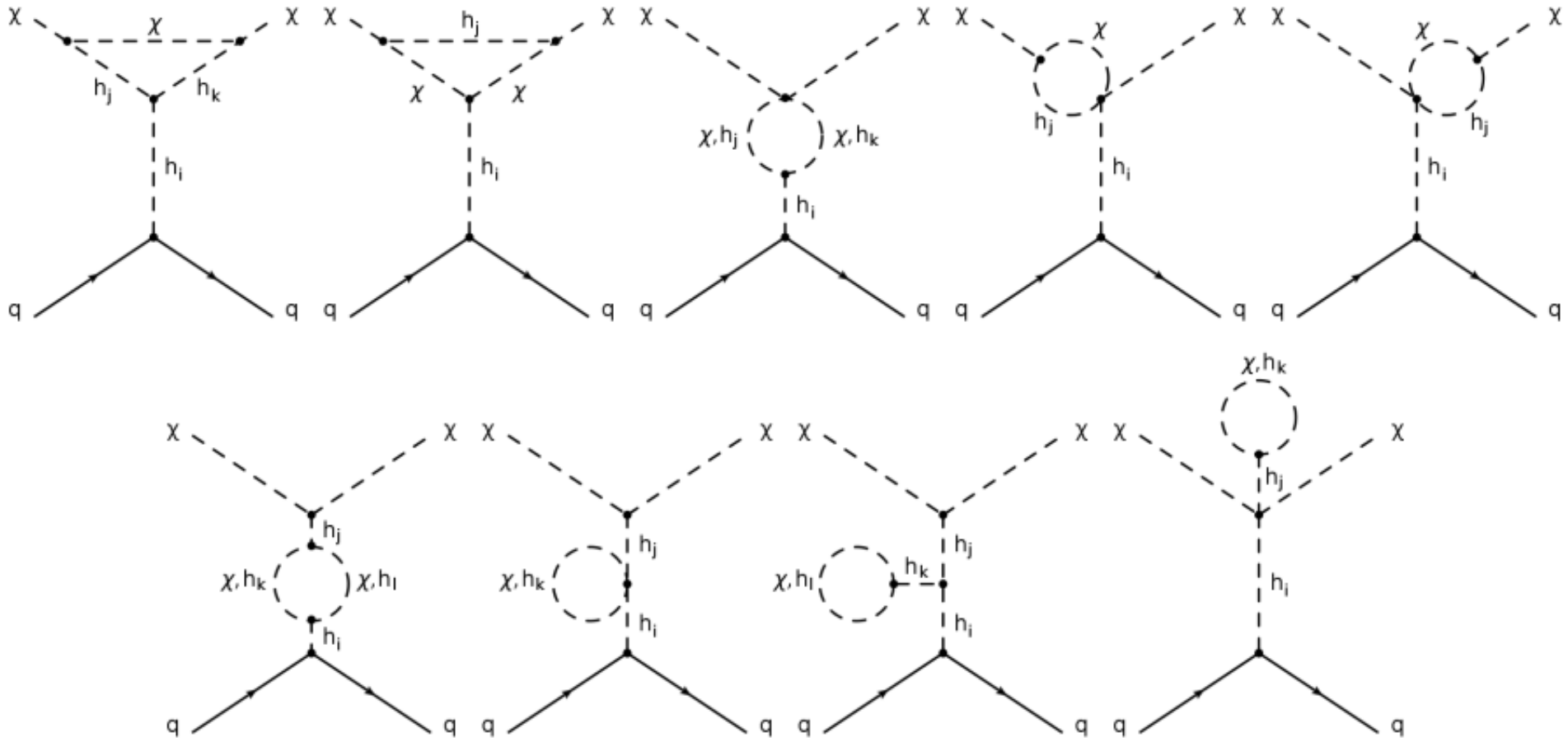

Renormalization

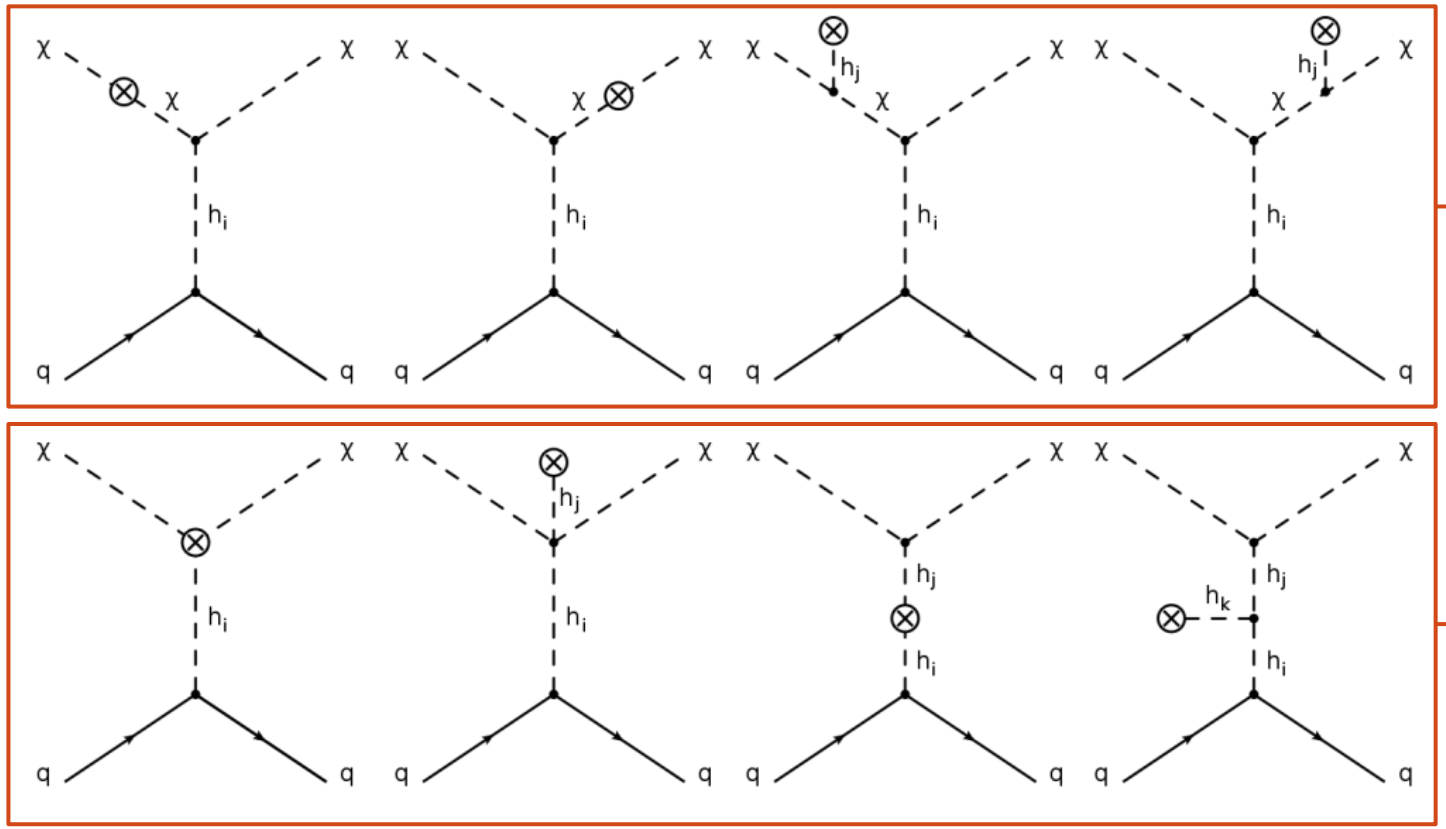

Proportional to tree-level amplitude

Contributions cancel between themselves

All counter-term contributions vanish → Amplitude at NLO is finite

[Azevedo, Duch, Grzadkowski, Huang, Iglicki, Santos, 2019]

Results

Parameter space scan

The scan of the parameter space was performed using the C++ code *ScannerS* which takes into consideration the most relevant theoretical and experimental constraints.

Theoretical constraints

- Perturbative unitarity
- Boundedness from below
- Vacuum stability

Experimental constraints

- Electroweak precision data
- Higgs couplings measurements
- Scalar exclusion limits
- Dark matter constraints
  - Relic abundance (Planck experiment)
  - Nucleon-DM cross section for direct detection (XENON1T experiment)

Type	m_{h_a}	$m_{h_b}, m_{h_c}, m_A, m_\chi$	$m_{H^\pm}$	$\alpha_{1,2,3}$	$\tan\beta$	M	v_S
I	125.09	[30,1000]	[150,1000]	$[-\pi/2, \pi 2]$	[1.5,10]	[20, 1000]	[30,1000]

Type	m_{h_a}	m_{h_b}, m_A	$m_{H^\pm}$	$m_{h_c,\chi}$	$\alpha_{1,2,3}$	$\tan\beta$	M	v_S
II	125.09	[200,1000]	[650,1000]	[30,1000]	$[-\pi/2, \pi 2]$	[1.5,10]	[450, 1000]	[30,1000]

[Coimbra, Sampaio, Santos, 2013]
[Mühlleitner, Sampaio, Santos, Wittbrodt, 2020]